



# Oxide cathode with perovskite structure for rechargeable lithium batteries

Yue Jin Shan <sup>a</sup>, Lique Chen <sup>b</sup>, Yoshiyuki Inaguma <sup>a</sup>, Mitsuru Itoh <sup>a</sup>,  
Tetsuro Nakamura <sup>a</sup>

<sup>a</sup> Research Laboratory of Engineering Materials, Tokyo Institute of Technology, 4259 Nagatsuta, Midori-ku, Yokohama 226, Japan

<sup>b</sup> Institute of Physics, Academia Sinica, PO Box 603, Beijing 100080, China

## Abstract

Lithium ions were electrochemically inserted into perovskite-type oxides  $\text{SrVO}_{3-\delta}$  and  $\text{La}_{0.50}\text{Li}_{0.37}\text{TiO}_{2.94}$  using galvanic cell:  $\text{Li}|1\text{ M LiClO}_4\text{ in PC}|\text{SrVO}_{3-\delta}$  or  $\text{La}_{0.50}\text{Li}_{0.37}\text{TiO}_{2.94}$ . It is found that the lattice parameters of  $\text{SrVO}_{3-\delta}$  will be increased and the discharge capacity of  $\text{SrVO}_{3-\delta}$  will be decreased as  $\delta$  increased. At the composition where all of A-site vacancies in  $\text{La}_{0.50}\text{Li}_{0.37}\text{TiO}_{2.94}$  are just occupied by the lithium ions, the lattice parameter shows a sudden increase. The chemical diffusion coefficients of lithium ions in  $\text{SrVO}_{3-\delta}$  and  $\text{La}_{0.50}\text{Li}_{0.37}\text{TiO}_{2.94}$  were determined to be the values in the range from  $10^{-8}$  to  $10^{-12}\text{ cm}^2\text{ s}^{-1}$ . Both oxides can be considered as a useful cathode of rechargeable lithium batteries. The charge/discharge characteristic can be improved by mixing of a small amount of carbon powder with the oxide.

**Keywords:** Rechargeable lithium batteries; Cathodes; Perovskite oxide

## 1. Introduction

Most of the cathode materials used in rechargeable lithium batteries possess hexagonal-layered structure or spinel structure. Many cathode materials are rather poor electronic conductors, for example, the electronic conductivity of most promising cathode  $\text{LiMn}_2\text{O}_4$  is  $1.4 \times 10^{-4}\text{ S cm}^{-1}$  at room temperature [1]. Usually, in practice 10 to 50 wt.% electronic conductors such as graphite or carbon black have to be mixed with active oxides [2]. As a result the energy density of the batteries is almost reduced. Therefore, cathode materials with both high ionic and high electronic conductivities are required for large energy density rechargeable batteries. In order to find high efficient cathode materials, we have paid attention to perovskite-type oxides.

In the  $\text{ABO}_3$  perovskite-type oxides, a transition metal element (B cation) occupies the centre of an octahedron which consist of six oxygen ions. Crystal systems and electronic conductivities of some perovskite-type oxides are shown in Table 1. It is easy to control their electric and magnetic properties by the substitution of A or B for another element. Furthermore, it is known that B cation can take different valence states in the range from 3 to 6 in the perovskite-type oxides. Therefore,

it is valuable to evaluate the possibility of lithium insertion into the perovskite-type oxide containing transition metal ions whose valences may decrease along with the lithium insertion.

First of all we will discuss the possibility whether perovskite-type structure has available sites and conduction passes for lithium ions to occupy and to migrate or not. Then, the maximum amount of inserted lithium ions, i.e., capacity, should be checked. In this study, two perovskite-type oxides  $\text{SrVO}_{3-\delta}$  and  $\text{La}_{0.5}\text{Li}_{0.37}\text{TiO}_{2.94}$  were subjected to lithium-insertion experiments.  $\text{SrVO}_{3-\delta}$  [4,10] and  $\text{La}_{0.50}\text{Li}_{0.37}\text{TiO}_{2.94}$  [9] are typical electronic conductors with one electron in the  $t_{2g}$  band ( $\sigma_{\text{ion}} \approx 10^3\text{ S cm}^{-1}$  at room temperature) and a high lithium ionic conductor with a negligible electronic conductivity ( $\sigma_{\text{electron}} \approx 10^3\text{ S cm}^{-1}$  at room temperature), respectively. The latter compound is expected to become an electronic conductor due to electron doping in the conduction band by the lithium insertion.

## 2. Experimental

$\text{SrVO}_{3-\delta}$  was prepared by the solid-state reaction method reported previously [11]. Some of the samples were heated either at 1073 K in Ar for 48 h or at 1673 K in  $\text{H}_2$  for 24 h to change the oxygen deficiency

Table 1  
Crystal systems and electronic conductivity of some perovskite-type oxides

Compounds	Crystal system	Electronic resistivity ( $\Omega$ cm at 300 K)	Ref.
SrTiO <sub>3</sub>	cubic	insulating	[3]
SrVO <sub>3</sub>	cubic	$1 \times 10^{-3}$	[4]
SrFeO <sub>3</sub>	cubic	$2 \times 10^{-3}$	[5]
SrRuO <sub>3</sub>	orthorhombic	$1 \times 10^{-3}$	[6]
SrMoO <sub>3</sub>	cubic	$10^{-4}$	[7]
LaMnO <sub>3</sub>	orthorhombic	semiconducting	[8]
(La <sub>0.51</sub> Li <sub>0.34</sub> )TiO <sub>2.94</sub>	cubic	insulating ( $\sigma_{Li^+} = 10^{-3}$ S cm <sup>-1</sup> )	[9]

$\delta$ . The results of this thermogravimetry analysis revealed that the oxygen deficiencies were found to be nearly zero in the former case and 0.13 in the latter case, respectively. La<sub>0.50</sub>Li<sub>0.37</sub>TiO<sub>2.94</sub> was prepared from La<sub>2</sub>O<sub>3</sub>(4 N), TiO<sub>2</sub>(4 N) and Li<sub>2</sub>CO<sub>3</sub>(3 N) according to the method given in Ref. [9]. Single-phased samples were used as cathodes for studying electrochemical lithium insertion and de-insertion.

Lithium ions were electrochemically inserted into perovskite oxides using a galvanic cell: Li|1 M LiClO<sub>4</sub> in PC|SrVO<sub>3- $\delta$</sub>  or La<sub>0.50</sub>Li<sub>0.37</sub>TiO<sub>2.94</sub> which consisted of a metallic lithium foil as anode, a piece of non-woven polypropylene cloth soaked with 1 M LiClO<sub>4</sub>-propylene carbonate (PC) (Mitsubishi Petrochemical Co.), and an oxide sheet as cathode. The sheet-type cathode was made of SrVO<sub>3- $\delta$</sub>  ( $0 < \delta < 0.13$ ) or La<sub>0.50</sub>Li<sub>0.37</sub>TiO<sub>2.94</sub> and 3 wt.% Teflon powder. The whole assembly was placed in a Teflon container covered with a brass screw cap on both ends. The lithium contents in the samples were controlled by the amount of electricity passed through the cell using a home-made galvanostat, and determined by inductively coupled plasma spectroscopy (ICP) using SEIKO SPS 1500 system. The identification of the phase and determination of lattice parameters of as-sintered and lithiated samples were carried out by Mac Science MXP<sup>18</sup> X-ray diffractometer. The chemical diffusion coefficients of lithium in SrVO<sub>2.95</sub> and La<sub>0.50</sub>Li<sub>0.37</sub>TiO<sub>2.94</sub> were measured with the galvanostatic intermittent titration technique (GITT) and a.c. impedance method, respectively. The impedance measurements were carried out in the three-electrode cell using a potentiostat (HOKUTO HA-301) and a frequency response analyser (NF Electronic Instrument 5720C) with a frequency range from  $10^{-2}$  Hz to  $10^2$  kHz. The working electrode was an La<sub>0.50</sub>Li<sub>0.37</sub>TiO<sub>2.94</sub> pellet (3 mm in diameter and 0.9 mm in thickness), both the counter and the reference electrodes were pure-lithium plates with about 3 cm  $\times$  2 cm and 1 cm  $\times$  2 cm, respectively, and the electrolyte was 1 M LiClO<sub>4</sub> in PC. The amplitude of the maximum signal was 10 mV. Some laboratory-type batteries were discharged/charged between the cutoff voltage of 1.2 and 3.0 V at  $23/5 \mu\text{A cm}^{-2}$  for La<sub>0.50</sub>Li<sub>0.37</sub>TiO<sub>2.94</sub> and  $45/8 \mu\text{A cm}^{-2}$  for SrVO<sub>2.95</sub>. All electrochemical ex-

periments were performed in a glove box filled with dry argon gas (5 N).

### 3. Results and discussion

#### 3.1. Behaviour of lithium-inserted SrVO<sub>3- $\delta$</sub>

Fig. 1 shows the cyclic voltammogram of Li|1 M LiClO<sub>4</sub> in PC|SrVO<sub>2.95</sub>. The cycling was performed between the voltages 1.0 and 3.2 V at a scanning rate of 4 mV s<sup>-1</sup>. Both insertion and de-insertion reactions could be observed clearly. After 80 cycles, the shape of the cycling voltammograms remained unchanged. This result indicates that the insertion and the de-insertion of lithium ions are reversible for SrVO<sub>2.95</sub>. Fig. 2 shows the continuous discharge curves of Li<sub>x</sub>SrVO<sub>3</sub>, Li<sub>x</sub>SrVO<sub>2.95</sub> and Li<sub>x</sub>SrVO<sub>2.87</sub> at  $13 \mu\text{A cm}^{-2}$  ( $0.34 \text{ mA g}^{-1}$ ). It is obvious that lithium ions can be electrochemically inserted into each of these samples. It is clearly shown in Fig. 2 that the discharge capacity decreases with the increase of oxygen deficiencies. This result can be interpreted by considering the difference in valency of the vanadium ions among these samples. The sample of SrVO<sub>3- $\delta$</sub>  contains oxygen vacancies of

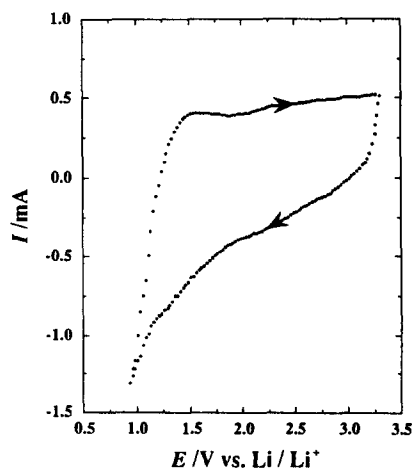


Fig. 1. Cyclic voltammogram of the cell Li|1 M LiClO<sub>4</sub>-PC|SrVO<sub>2.95</sub> between 1.0 and 3.2 V at a scanning rate of 4 mV s<sup>-1</sup>.

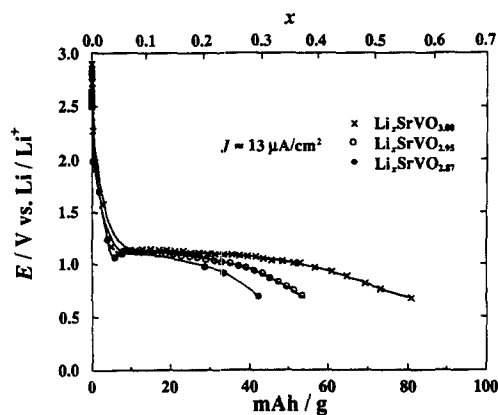


Fig. 2. Continuous discharge curves for  $\text{Li}_x\text{SrVO}_3$ ,  $\text{Li}_x\text{SrVO}_{2.95}$  and  $\text{Li}_x\text{SrVO}_{2.87}$  at  $13 \mu\text{A cm}^{-2}$  ( $0.34 \text{ mA g}^{-1}$ ).

the amount  $\delta$  together with  $\text{V}^{3+}$  cations of the amount  $2\delta$  to preserve charge electroneutrality, and then it can be written formally as a solid solution  $\text{Sr}(\text{V}_{1-2\delta}^{4+}\text{V}_{2\delta}^{3+})\text{O}_{3-\delta}$ . So, the trivalent vanadium ions should increase as  $\delta$  increases. On the other hand, lithium insertion can be considered as a formation process of a solid solution of  $\text{Li}_x\text{SrVO}_{3-\delta}$ . If a lithium ion was electrochemically inserted into  $\text{SrVO}_{3-\delta}$  crystals, then it must gain an electron simultaneously to preserve electroneutrality. In this case, it is obvious that vanadium(IV) ion is reduced to vanadium(III) ion. Thus, the trivalent vanadium ions increase as the amount of inserted lithium ions ( $x$ ) increases. Therefore, the discharge capacities should decrease with increasing  $\delta$  and depends on the initial amount of  $\text{V}^{4+}$  ions in the sample since the average valence of B-site ions in the perovskite structure cannot take a value smaller than 3.0. The amount of the inserted lithium  $x$  in the formula  $\text{Li}_x\text{SrVO}_3$  is considered to reach nearly unity, giving the ideal capacity  $140 \text{ mAh g}^{-1}$ . According to the results of X-ray powder diffraction, all the lithiated samples were found to have perovskite structure. A single phase was obtained for  $\text{Li}_x\text{SrVO}_{3-\delta}$  (except  $\text{Li}_{0.56}\text{SrVO}_{2.95}$ ). For  $\text{Li}_{0.56}\text{SrVO}_{2.95}$ , formation of two phases with different lithium contents were confirmed. Fig. 3 shows the lattice parameter versus lithium content in  $\text{Li}_x\text{SrVO}_{3-\delta}$ . The lattice parameters slightly increase in  $\text{Li}_x\text{SrVO}_{3.00}$ , and show a minimum in  $\text{Li}_x\text{SrVO}_{2.95}$ . From the geometrical consideration for the imaginary ionic  $\text{SrVO}_3$ , we have concluded that lithium ions can occupy the largest interstitial space, 3c-site, in the cubic perovskite structure. The appearance of the minimum for the oxygen-deficient samples may be due to the interaction between lithium ions and oxygen vacancies. The chemical diffusion coefficient for  $\text{SrVO}_{2.95}$  was found to be in the order of  $10^{-8} \text{ cm}^2 \text{ s}^{-1}$  by the GITT method. This value is larger and comparable with the chemical diffusion coefficients of lithium in  $\text{TiS}_2$  ( $1.1 \times 10^{-8}$ – $8.1 \times 10^{-12} \text{ cm}^2 \text{ s}^{-1}$ ) determined by the same method [12].

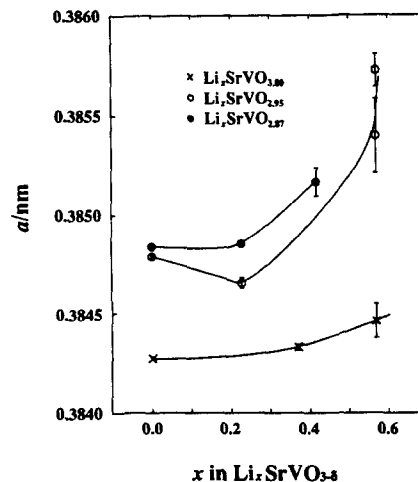


Fig. 3. Variation of lattice parameters with lithium content in the sample  $\text{Li}_x\text{SrVO}_{3-\delta}$  ( $0 \leq \delta \leq 0.13$ ).

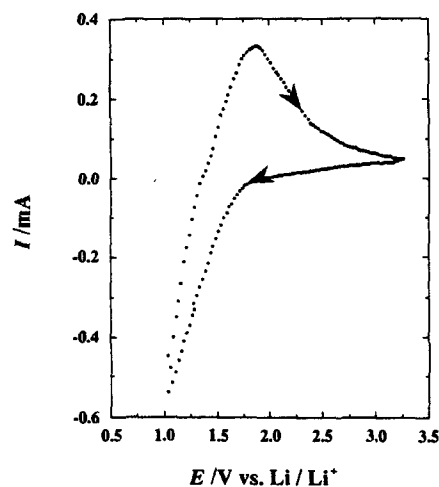


Fig. 4. Cyclic voltammogram of the cell  $\text{Li}|1 \text{ M LiClO}_4\text{-PC}|\text{La}_{0.50}\text{Li}_{0.37}\text{TiO}_{2.94}$  between 1.0 and 3.2 V at a scanning rate of  $4 \text{ mV s}^{-1}$ .

### 3.2. Behaviour of lithium-inserted $\text{La}_{0.50}\text{Li}_{0.37}\text{TiO}_{2.94}$

The cyclic voltammogram of  $\text{La}_{0.50}\text{Li}_{0.37}\text{TiO}_{2.94}$  is shown in Fig. 4. The current voltage curves suggest the possibility of these materials upon de-insertion and insertion of  $\text{Li}^+$  ions in the voltage range from 1.0 to 3.2 V versus  $\text{Li/Li}^+$ , at a scanning rate of  $4 \text{ mV s}^{-1}$ . Even after 80 cycles, no change was found in the shapes and positions of the oxidation and reduction peaks, given in Fig. 4. Therefore, it is considered that the insertion and de-insertion of lithium ions are reversible for  $\text{La}_{0.50}\text{Li}_{0.37}\text{TiO}_{2.94}$ . Fig. 5 shows the continuous discharge curve of  $\text{Li}_x\text{La}_{0.50}\text{Li}_{0.37}\text{TiO}_{2.94}$  at  $13 \mu\text{A cm}^{-2}$  ( $0.34 \text{ mA g}^{-1}$ ). The cell voltage decreased linearly with the lithium insertion. The slope of the curve changed at point P. It is considered that the inserted lithium ions occupy two different positions in the lattice of  $\text{La}_{0.50}\text{Li}_{0.37}\text{TiO}_{2.94}$ . At point P, the amount of inserted

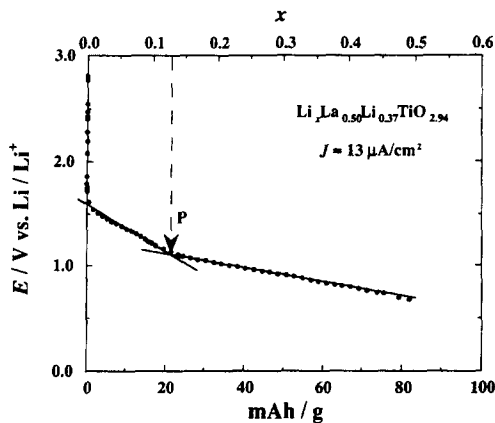


Fig. 5. Continuous discharge curve of  $\text{Li}_x\text{La}_{0.50}\text{Li}_{0.37}\text{TiO}_{2.94}$  at  $13 \mu\text{A cm}^{-2}$  ( $0.34 \text{ mA g}^{-1}$ ).

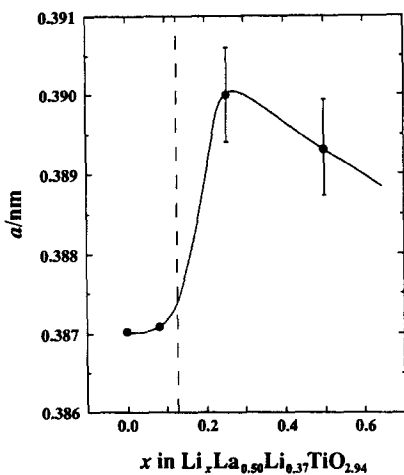


Fig. 6. Variation of the lattice parameters with lithium content in the sample  $\text{Li}_x\text{La}_{0.50}\text{Li}_{0.37}\text{TiO}_{2.94}$ .

lithium ions  $x$  was about 0.13 and equal to the amount of A-site vacancies. This result indicated that lithium ions were inserted into A-site vacancies until they were occupied by lithium ions (point P). Beyond P point, lithium ions were inserted into 3c-site that is similar to the case of lithium-inserted  $\text{SrVO}_{3-\delta}$  with no A-site vacancies. The amount of the inserted lithium  $x$  in the formula  $\text{La}_{0.50}\text{Li}_{0.37}\text{TiO}_{2.94}$  are considered to reach nearly unity, giving the ideal capacity  $160 \text{ mAh g}^{-1}$ . The lattice parameters versus the amounts of inserted lithium ions are plotted in Fig. 6. Before A-site vacancies were full of inserted lithium ions, the lattice parameters changed somewhat. As soon as lithium ions were inserted into 3c-site, the lattice parameters increased rapidly, being close to that of  $\text{LaTiO}_3$  (0.392 nm). Typical a.c. impedance spectra of  $\text{Li}_x\text{La}_{0.52}\text{Li}_{0.35}\text{TiO}_{2.96}$  with various  $x$  values are shown in Fig. 7. The a.c. impedance responses can be modelled by the Randles equivalent circuit [13]. In Fig. 7, the impedance diagrams exhibit two features: (i) semicircles in the high frequency range being related to a charge-transfer process, and (ii) straight lines in

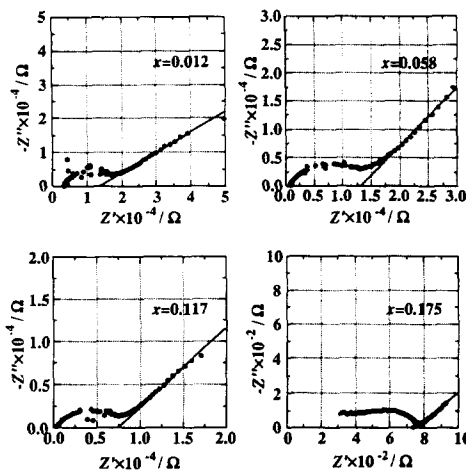


Fig. 7. Typical a.c. impedance diagrams in the complex plane for  $\text{Li}_x\text{La}_{0.52}\text{Li}_{0.35}\text{TiO}_{2.96}$ :  $x = 0.012$ ;  $x = 0.058$ ;  $x = 0.117$ , and  $x = 0.175$ .

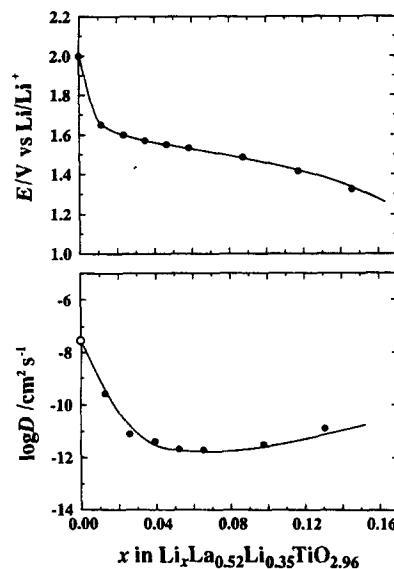


Fig. 8. Open-circuit voltages and chemical diffusion coefficients of lithium vs. lithium content in the sample of  $\text{Li}_x\text{La}_{0.52}\text{Li}_{0.35}\text{TiO}_{2.96}$ .

the low frequency range, being characteristic of diffusion process. The decrease in the radius of the semicircle with  $x$  indicates the increase in electronic conductivity caused by the electron doping in the conduction band, i.e., reduction of titanium(IV) to titanium(III). The chemical diffusion coefficient of lithium,  $D$ , was calculated from the low frequency limiting resistance by using the  $\sqrt{D} = Z_w V_m / nFS (dE/dx)$  equation [14]. Fig. 8 shows the open-circuit voltage and the chemical diffusion coefficients versus lithium in the sample of  $\text{Li}_x\text{La}_{0.52}\text{Li}_{0.35}\text{TiO}_{2.96}$ . The data of  $\text{La}_{0.52}\text{Li}_{0.35}\text{TiO}_{2.96}$  ( $x = 0$ ) was determined by the Nernst-Einstein equation [15] using the conductivity data, and was in good agreement with the extrapolated value of the impedance data. As can be seen in Fig. 8, the diffusion coefficient

$D$  decreased with increasing  $x$  in the range  $x < 0.05$ , and turned to increase in the range  $x > 0.05$ . In the range  $x < 0.05$ , the decrease in diffusion coefficient  $D$  with increasing  $x$  may be caused by a decrease in the number of unoccupied sites (A-site vacancies) of lithium ions. In the range  $x > 0.05$ , the increase in the  $D$  value may be correlated to the expansion of the lattice (Fig. 6) with  $x$ .

### 3.3. Discharge/charge characteristics

Discharge/charge cycling curves of the laboratory-type battery using  $\text{SrVO}_{2.95}$  and  $\text{La}_{0.50}\text{Li}_{0.37}\text{TiO}_{2.94}$  as cathodes are shown in Figs. 9 and Fig. 10, respectively. Discharge/charge cycling can be continued without any conductive additives because  $\text{SrVO}_{2.95}$  and lithiated  $\text{La}_{0.50}\text{Li}_{0.37}\text{TiO}_{2.94}$  possess electronic conductivity as described above. But, the capacities were small and the losses were big. The reasons for these phenomena have not been yet clear. The upturn in the charge curve for  $\text{Li}_x\text{La}_{0.50}\text{Li}_{0.37}\text{TiO}_{2.94}$  may be caused by a decrease in the electronic conductivity at the surface of the sample caused by the oxidation of titanium ions from 3+ to 4+ (insulating state). The discharge/charge characteristic of the laboratory-type battery can be obviously

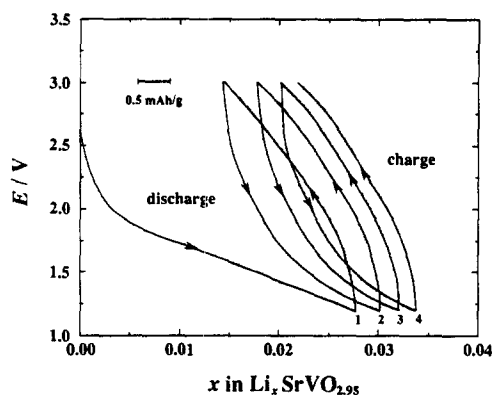


Fig. 9. Discharge/charge cycling curves of the laboratory-type battery using  $\text{SrVO}_{2.95}$  as cathode.

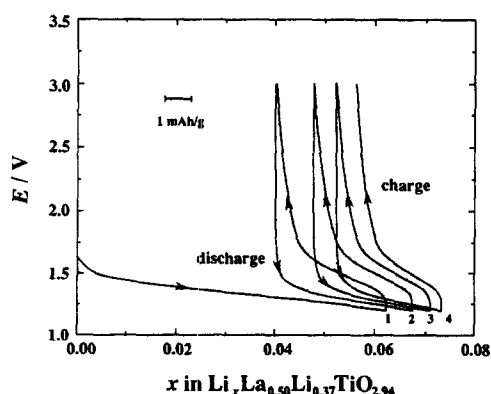


Fig. 10. Discharge/charge cycling curves of the laboratory-type battery using  $\text{La}_{0.50}\text{Li}_{0.37}\text{TiO}_{2.94}$  as the cathode.

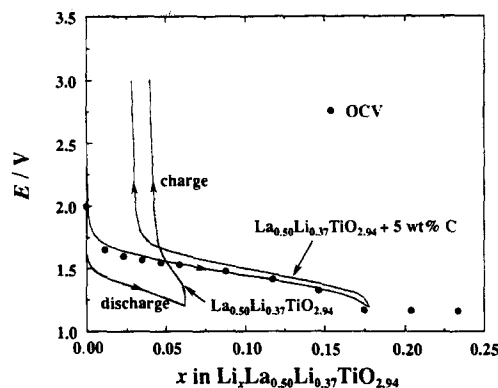


Fig. 11. Comparison of the first discharge/charge curves for the laboratory-type batteries using  $\text{La}_{0.50}\text{Li}_{0.37}\text{TiO}_{2.94}$  and  $\text{La}_{0.50}\text{Li}_{0.37}\text{TiO}_{2.94} + 5 \text{ wt.}\% \text{ C}$  as cathode; (●) denotes open-circuit voltage measured for a three-electrode cell.

improved by mixing a small amount of carbon black (5 wt.%) with  $\text{La}_{0.50}\text{Li}_{0.37}\text{TiO}_{2.94}$  (see Fig. 11). Therefore, we can estimate that the role of mixed carbon is not only an enhancement of electronic conductivity in the sample sheet but it gives also catalytic-active places for the electrochemical reaction and diffusion of lithium ions. Further experiments are needed to elucidate the role of mixing of carbon powders with the electronic conductive cathodes.

## 4. Conclusions

Lithium ions could be electrochemically inserted into and de-inserted from perovskite-type oxides  $\text{SrVO}_{3-\delta}$  or  $\text{La}_{0.50}\text{Li}_{0.37}\text{TiO}_{2.94}$ . From the results, it can be suggested that the inserted lithium ions first occupied A-site vacancies then 3c-sites. The lithium insertion leads to the reduction of transition metal ion (B cation) in electroneutrality and the increase in lattice parameter. The chemical diffusion coefficient of lithium for  $\text{SrVO}_{3-\delta}$  was found to be in the order of  $10^{-8} \text{ cm}^2 \text{ s}^{-1}$  and that of  $\text{Li}_x\text{La}_{0.50}\text{Li}_{0.37}\text{TiO}_{2.94}$  in the range from  $10^{-8}$  to  $10^{-12} \text{ cm}^2 \text{ s}^{-1}$  ( $0 < x < 0.225$ ). The discharge/charge characteristics of the laboratory-type battery can be improved by mixing a small amount of carbon black (5 wt.%) with  $\text{La}_{0.50}\text{Li}_{0.37}\text{TiO}_{2.94}$ .

## References

- [1] L. Chen and J. Schoonman, *Solid State Ionics*, 67 (1993) 17.
- [2] N. Kumagai, S. Tanifuji and K. Tanno, *J. Power Sources*, 35 (1991) 313.
- [3] J.F. Schooley, W.R. Hos and M.L. Cohen, *Phys. Rev. Lett.*, 12 (1964) 474.
- [4] M. Onoda, H. Ohda and H. Nakasawa, *Solid State Commun.*, 79 (1991) 281.

- [5] J.B. Macchesney, R.C. Sherwood and J.F. Potter, *J. Chem. Phys.*, 43 (1965) 1907.
- [6] Y. Noro and S. Miyagata, *J. Phys. Soc. Jpn.*, 27 (1969) 518.
- [7] S. Hayashi, R. Aoki and T. Nakamura, *Mater. Res. Bull.*, 14 (1979) 409.
- [8] A. Daoudi, A. Benabad, R. Salmon and G.L. Felm, *J. Solid State Chem.*, 22 (1977) 121.
- [9] Y. Inaguma, L. Chen, M. Itoh, T. Nakamura, T. Uchida, M. Ikuta and M. Wakihara, *Solid State Commun.*, 86 (1993) 689.
- [10] M. Itoh, M. Shikano, H. Kawaji and T. Nakamura, *Solid State Commun.*, 80 (1991) 545.
- [11] Y.J. Shan, L. Chen, Y. Inaguma, M. Itoh, T. Nakamura, *Solid State Ionics*, 70/71 (1994) 429.
- [12] R.D. Shannon, *Acta Crystallogr., Sect. A*, 32 (1976) 51.
- [13] J.E.B. Randles, *Discuss. Faraday Soc.*, 1 (1947) 11.
- [14] C. Ho, I.D. Raistrick and R.A. Huggins, *J. Electrochem. Soc.*, 127 (1980) 343.
- [15] A.R. West, *Solid State Chemistry and its Applications*, Wiley, New York, 1984, p. 462.